Journal of Modern Physics, 2015, 6, 1803-1813
Published Online October 2015 in SciRes. http://www.scirp.org/journal/jmp
http://dx.doi.org/10.4236/jmp.2015.613184

Effect of Heat Treatment on the Nanoscale Structure and Optical Properties of Cd_2SnO_4 Thin Films Deposited by RF Magnetron Sputtering

Ateyyah M. Al-Baradi

Department of Physics, Taif University, Taif, Kingdom of Saudi Arabia
Email: thobyani@yahoo.com

Received 21 August 2015; accepted 18 October 2015; published 21 October 2015

Abstract

Cadmium tin oxide Cd_2SnO_4 thin films with a thickness of 228.5 nm were prepared by RF magnetron sputtering technique on glass substrates at room temperature. AFM has been utilized to study the morphology of these films as a function of annealing temperature at the nanoscale. The optical properties of these films, such as the transmittance, $T(\lambda)$, and reflectance, $R(\lambda)$, have been studied as a function of annealing temperature. The optical constants, such as optical energy gap, width of the band tails of the localized states, refractive index, oscillatory energy, dispersion energy, real and imaginary parts of both dielectric constant and optical conductivity have been found to be affected by changing the annealing temperature of the films.

Keywords

Thin Films, Atomic Force Microscope, Transmittance, Reflectance, Optical Energy Gap, Optical Conductivity

1. Introduction

Tin oxide SnO_2, Indium oxide InO_3, and Zink oxide ZnO are good examples of degenerate semiconductors which are highly transparent and conducting in the family of binary transparent conducting oxides (TCOs). However, ternary oxide TCOs such as Zn_2SnO_4 [1], $CdInO_4$ [2], $ZnGa_2O_4$ [3] and Cd_2SnO_4 [4] have eminent properties required for a transparent conducting oxide. It is reported that Cd_2SnO_4 thin films show electrical resistivity of about 10^{-4} Ω·cm, high transmission (>90%) in the visible region and smoother surface than conven-

How to cite this paper: Al-Baradi, A.M. (2015) Effect of Heat Treatment on the Nanoscale Structure and Optical Properties of Cd_2SnO_4 Thin Films Deposited by RF Magnetron Sputtering. *Journal of Modern Physics*, **6**, 1803-1813.
http://dx.doi.org/10.4236/jmp.2015.613184

tional SnO_2 TCO films [5] [6]. This aspect makes Cd_2SnO_4 films an important material for the application as electrode materials in photovoltaic devices. It is known that transparent conducting oxides are a class of material that transmit visible radiation and conduct electricity. It is found that it has wide applications as transparent electrode, flat panel display, heat reflective coatings on energy-efficient windows, and electrochromics in smart windows [7]-[9] solar cells [10] [11], abrasion resistance coatings [12], corrosion resistant coatings [13], gas sensors [14], ohmic contacts to surface-emitting lasers [15] [16], ohmic contacts to photodetectors [17] [18], Shottky contacts to photodetectors [19]-[23], and heat mirrors for energy efficient windows and light bulbs [24]. The properties of these films are highly dependent on the technique of deposition and the substrate upon which they are deposited. Cadmium oxide is an n-type semiconductor, with direct band gap of between 2.4 and 2.7 eV, and has a poor optical transmittance in the visible spectral region [25]. Tin oxide (SnO_2) is an n-type semiconductor, which possesses perfect physical properties. In addition, it shows high variations of electrical resistance in the presence of oxidizing and reducing gases. Thin tin oxide films exhibit high optical transparency (>80%) in the visible region [26]. In a previous study [27], it is found that the direct optical gap of Cd_2SnO_4 thin films decreases from 3.2 eV to 3.13 eV with increasing γ-irradiation dose up to 100k Gy. The direct optical gap which is calculated from optical absorption measurements is higher than that obtained from Photoluminescence (PL) measurements $E_g^{PL} = 2.82$ eV [27]. It is also found that the obtained values of E_g^d are independent on the film thickness in the utilized thickness range and that the discrepancy is within the estimated experimental errors $E_g^d = 2.91$ eV [28].

The present work shows the possibilities of successfully prepare Cadmium Stannate (Cd_2SnO_4) thin films using RF sputtering technique. The obtained thin films have been studied under various conditions especially as a function of annealing temperature that to our knowledge has been paid a little attention.

2. Experimental Technique

Thin films of Cd_2SnO_4 with thickness of 228.5 nm are prepared using a target constitute of (Cd:SnO_2 ratio of 2:1), the targets was purchased from Cathay Advanced Materials Limited (China). The films were deposited onto ultrasonically cleaned glass substrates using UNIVE 350 sputtering unit with RF power model Turbo drive TD20 classic (Leybold), RF power model CESAR, RF power generator and rate thickness monitor model INFICON SQM-160. The deposition conditions were: base pressure of about 2×10^{-3} Pa, substrate to target distance of 10 Cm, RF power of 150 W, self bias 400 V, deposition pressure of 2 Pa, argon flow rate of 10 SCCM. The substrate temperature during deposition was kept at room temperature. The prepared Cd_2SnO_4 films were annealed in air at different temperatures in the range from 150˚C to 550˚C. Atomic force microscope model (Veeco-di Innova Model-2009-AFM-USA) was used to obtain the topographical images of the film surface and to describe the changes of the grain size with changing the annealing temperature. The optical transmittance, $T(\lambda)$, and reflectance, $R(\lambda)$, of the films under investigation were measured by means of a computer programmable Jasco V-570 (Japan) double beam spectrophotometer in the wavelength range from 200 to 2000 nm at normal incidence. In case of reflectivity measurement, an additional attachment model ISN-470 was used. The absorption coefficient α of the films was determined directly from the spectrophotometer measurements using the formula [29]:

$$\alpha = \frac{2.303}{d}\mathrm{Log}_{10}\left(\frac{1-R}{T}\right), \tag{1}$$

where d is the film thickness, T is the transmittance and R is the reflectance of the films.

The optical energy band gap E_g was estimated from the optical measurements by analyzing the optical data with the expression for the optical absorption coefficient α and the photon energy $h\upsilon$ using the following equation:

$$(\alpha h\upsilon) = A\left(h\vartheta - E_g\right)^n, \tag{2}$$

where h is the Planck's constant and A is a constant. E_g was obtained by extrapolating the linear portion of the plots of $(\propto h\vartheta)^{1/n}$ versus ($h\nu$) to $\alpha = 0$. The refractive index n was calculated from the following equation:

$$n = \frac{1+R}{1-R} \pm \left[\left(\frac{R+1}{R-1}\right)^2 - \left(1+k^2\right)\right]^{1/2}, \tag{3}$$

where $k = \alpha\lambda/4\pi$ is the extinction coefficient and λ is wavelength of the incident light.

3. Results and Discussions

Figures 1(a)-(e) show the morphology of annealed Cd_2SnO_2 thin films with a thickness of 228.5 nm at 150˚C, 250˚C, 380˚C, 450˚C and 550˚C obtained by AFM using tapping mode. AFM images in **Figure 1** show that the coated films consist of grains that increase in size with increasing the annealing temperature. The grain size of the investigated films was measured using grain size analyzer in another stage during the investigations of surface topology of the film sample. The obtained values of the grain size increased from 168 nm at 150˚C to 230 nm at 550˚C (see **Table 1**). **Table 1** also shows the increase of the root mean square roughness (RMS) from 2.84 nm at 150˚C to 33.19 nm at 550˚C.

The transmittance, $T(\lambda)$, and reflectance, $R(\lambda)$, spectra for the annealed Cd_2SnO_4 thin films of the same thickness 228.5 nm at different annealing temperatures (150˚C, 250˚C, 380˚C, 450˚C and 550˚C) are shown in **Figure 2**. It is clear that the change in the transmittance increases with increasing annealing temperature may be due to some improvements in film properties. On the other hand, the transmittance increases with increasing the incident photon wavelength in the optical spectra range, after that it continued increasing till wavelength of 900 nm and then it seems to be independent on photon wavelength. The maximum value of the transmittance was found to be at a wavelength of 1200 nm and varies from 95% to 98% for the annealed thin films (see **Figure 2**). **Figure 2** also shows typical reflection spectra for annealed Cd_2SnO_4 films (228.5 nm thick) at different temperatures (150˚C, 250˚C, 380˚C, 450˚C and 550˚C). The transmission loss can be seen at longer wavelengths that can be interpreted as due to photon-electron interaction by which photons can be scattered. Losses occurs a result of both reflection and absorption. Reflection in this region is not strictly a surface phenomenon. Reflection from the bulk of the material can occur, provided that the electron escapes the surface. If the scattered electron does not escape the surface then it can be concluded that it has been absorbed [30].

Figure 3 shows the spectral behavior of the absorption coefficient α for annealed Cd_2SnO_4 thin films at 150˚C, 250˚C, 380˚C and 450˚C and 550˚C, where $\alpha = 4\pi k/\lambda$. It can be noticed that the absorption edge of α has a trend to decrease with increasing the annealing temperature.

The optical energy gap is estimated from the optical measurements by analyzing the optical data with the expression for the optical absorbance, and the photon energy, $h\vartheta$, using Equation (2). The optical band gap can be obtained by extrapolating the linear portion of the plots of $(\alpha h\vartheta)1/n$ versus $h\vartheta$ to $\alpha = 0$. Using the value n = 1/2, the relation found to be straight line as shown in **Figure 4** indicating a direct optical transition. **Figure 4** reveals that the optical gap of the Cd_2SnO_4 thin films (228.5 nm thick) has the values 3.17, 3.19, 3.18, 3.16 and 3.29 eV for the annealed films at 150˚C, 250˚C, 380˚C, 450˚C and 550˚C, respectively, indicating that the optical gap seems to be increased with increasing the annealing temperature. It is reported that the optical gap of the Cd_2SnO_4 thin films is around 3 eV [30], which is in consistent more or less with the present results. The increase in the band gap energy with increasing the annealing temperature can be attributed to the Burstein-Moss shift in which the absorption edge shifts towards higher energy with an increase in carrier concentration [31] [32]. Increasing the optical band gap E_g with increasing the annealing temperature can be explained as follows; the unsaturated defects are gradually annealed out producing a larger number of saturated bonds leading to a decrease in the density of localized states and consequently the optical gap increases [33].

To calculate the width of the band tails E_e of the localized states, the following equation [34] can be used:

$$\alpha(\omega) = \alpha_o(\omega)\mathrm{e}^{h\nu/E_e}, \tag{4}$$

where $\alpha_o(\omega)$ is a constant, h is the Plank's constant. **Figure 5** shows the Ln $\alpha(\omega)$ versus $(h\nu)$, in which the slope can be used to calculate E_e for the annealed films. The calculated values of the band tails of the localized states E_e from **Figure 5** have been found to be larger than 0.05 eV for all annealed films at 150˚C, 250˚C, 380˚C and 450˚C and 550˚C. This behavior of decreasing the values of E_e with increasing annealing temperature agrees well with our results of increasing that reveal E_{op} with increasing the annealing temperature. Because the values of E_e are very much larger than 0.05 eV, Tauc's model based on electronic transitions between localized states in the band edge tails may well be valid in our systems [35].

The variation of the refractive index with the wavelength is shown in **Figure 6** indicating the decrease of refractive index with increasing the wavelength, which represents the normal dispersion. The effect of annealing is obvious from **Figure 6**, where the refractive index decreases with increasing the annealing temperature that may

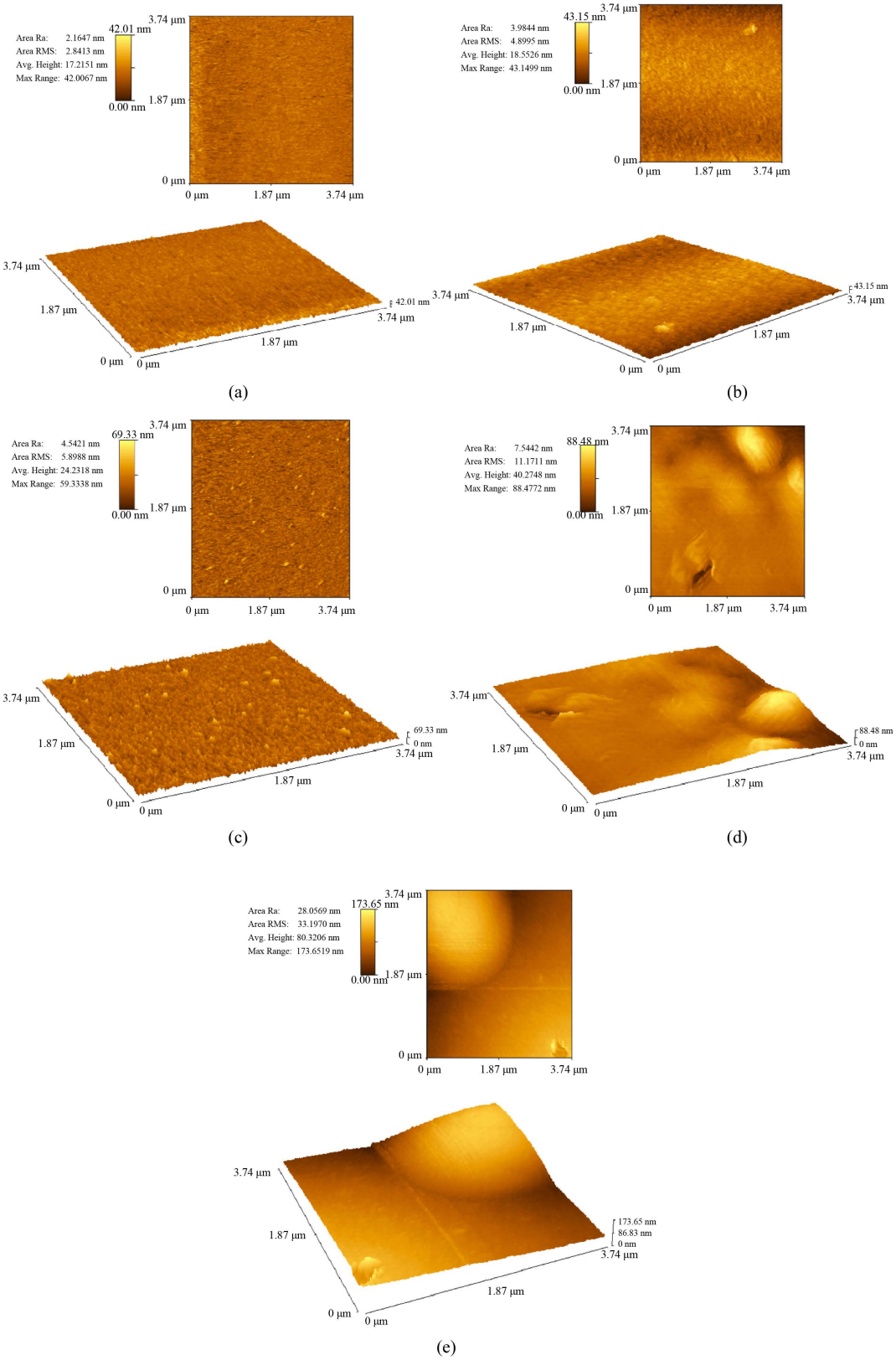

Figure 1. AFM images for Cd_2SnO_4 thin film of thickness 228.5 nm annealed at (a) 150˚C, (b) 250˚C, (c) 380˚C, (d) 450˚C and (e) 550˚C.

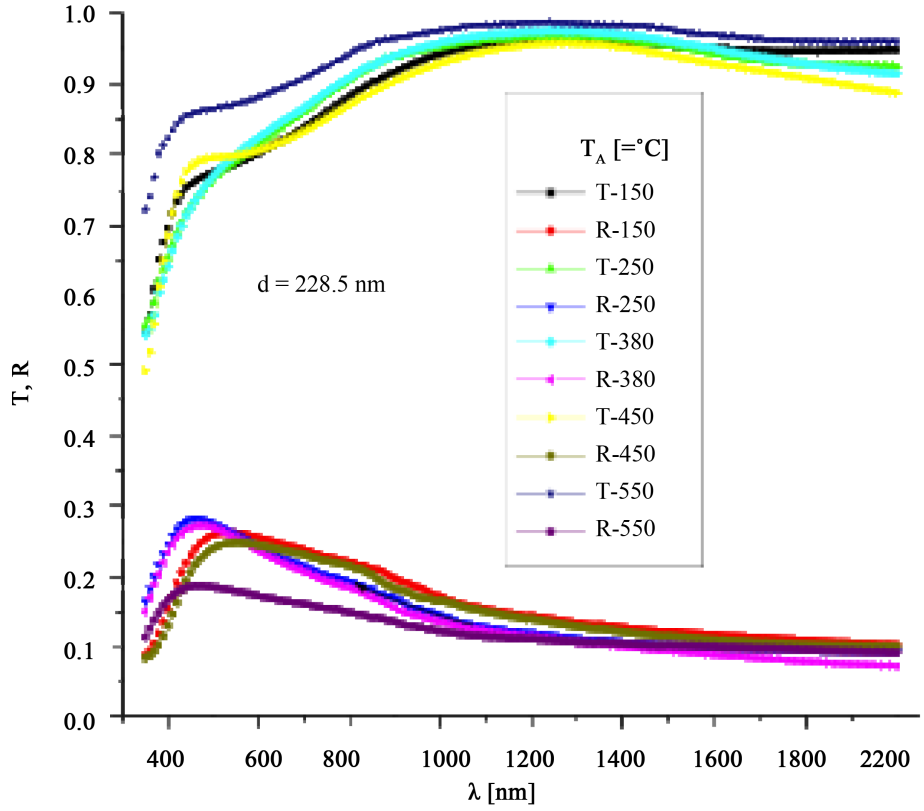

Figure 2. The optical transmittance $T(\lambda)$ and reflectance $R(\lambda)$ for the annealed Cd_2SnO_4 thin films.

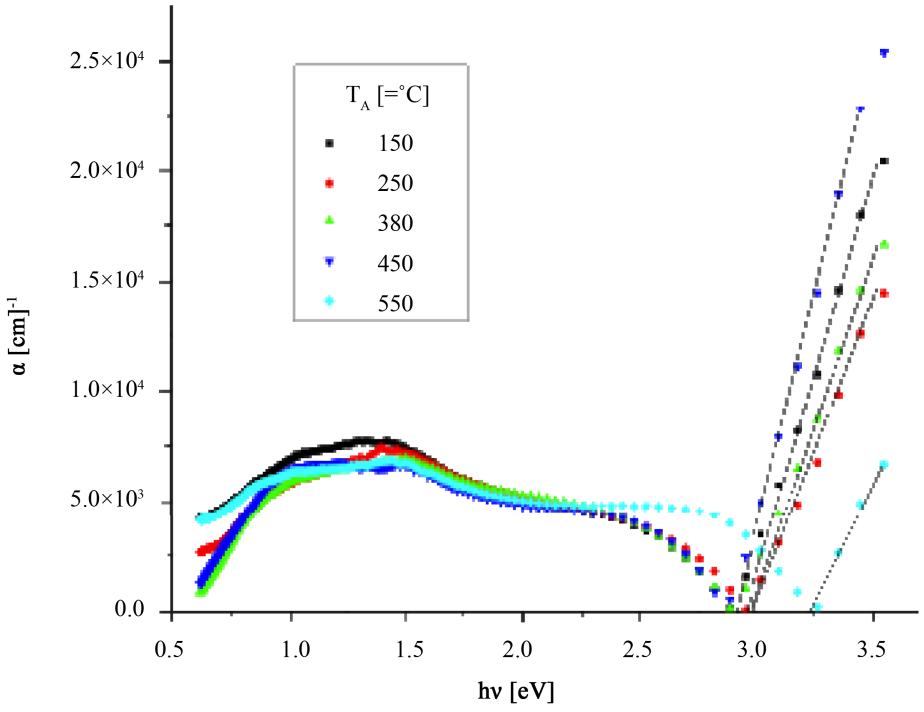

Figure 3. The spectral behaviour of the absorption coefficient, α ($h\nu$), for annealed Cd_2SnO_4 thin films.

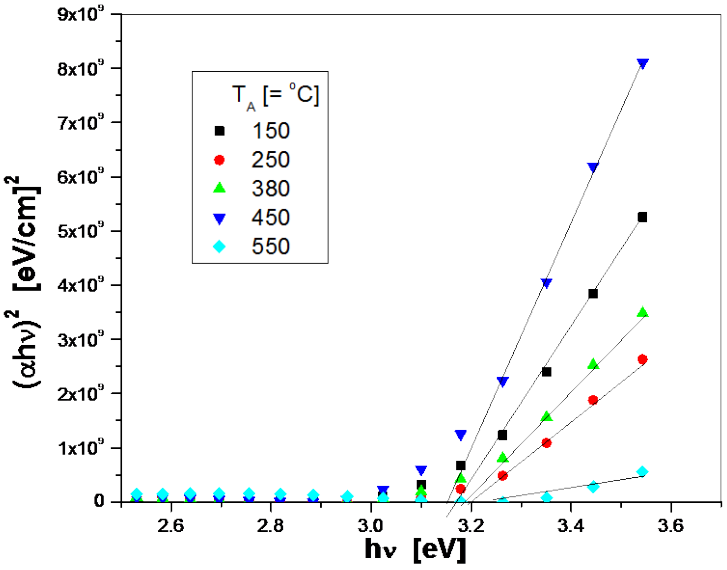

Figure 4. The relation between $(\alpha h\nu)^2$ and photon energy $(h\nu)$ for the annealed Cd_2SnO_4 thin films.

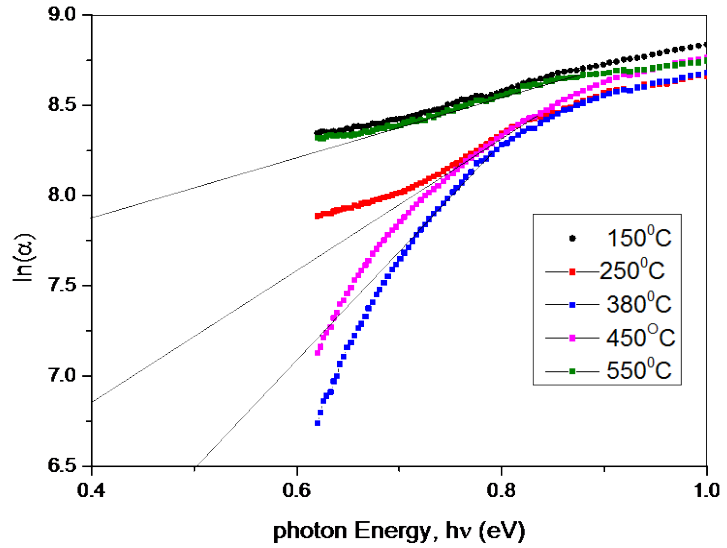

Figure 5. A plot of $\ln(\alpha)$ versus $h\nu$ for the annealed Cd_2SnO_4 thin films.

be attributed to the decrease in the packing density with increasing annealing temperature [33].

In the transparent region, the obtained data of refractive index, n, can be analyzed to obtain the lattice dielectric constant, ε_L, via a procedure describes the contribution of the free carriers and the lattice vibration modes of the dispersion. The relationship between the real dielectric constant, ε_1, and the wavelength, λ, in normal dispersion region is given by [36]:

$$\varepsilon_1 = n^2 = \varepsilon_L - \frac{e^2 N}{4\pi^2 \varepsilon_o m^* c^2}\lambda^2, \tag{5}$$

where e is the elementary charge, ε_o is the permittivity of free space and, N/m^* is the ratio of free carrier concentration to the effective mass of electrons. **Figure 7** shows the relationship between n^2 and λ^2 for the annealed Cd_2SnO_4 films. It can be noticed that the dependence of $(n^2 = \varepsilon_1)$ on λ^2 is linear atlonger wavelengths. Extrapolating these linear parts to zero wavelength gives the value of ε_L and from the slopes of these linear parts the

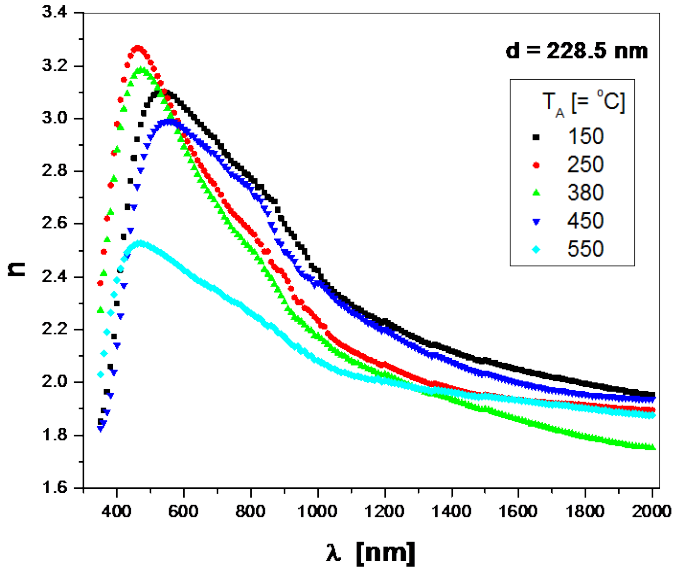

Figure 6. The spectral behavior of the real part of refractive index, $n(\lambda)$, for the annealed Cd_2SnO_4 thin films.

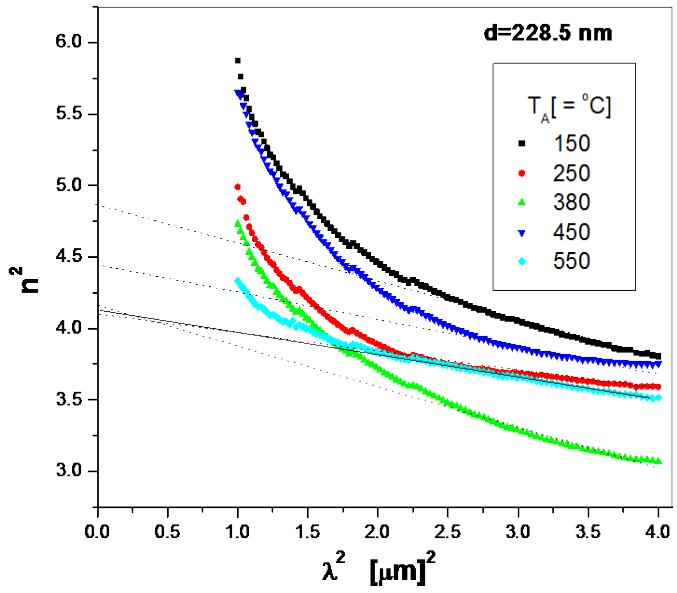

Figure 7. The relation between n^2 and λ^2 for the annealed Cd_2SnO_4 thin films.

Table 1. The average root mean square roughness, average height and maximum height for annealed Cd_2SnO_4 thin films obtained from AFM measurements.

Annealing temperature (˚C)	Average particle size (nm)	Root mean square roughness (RMS) (nm)	Average height (nm)	Maximum height (nm)
150	168	2.84	17.22	42.01
250	171	4.89	17.22	43.15
380	195	5.89	24.23	63.33
450	211	11.17	40.27	88.48
550	230	33.19	80.32	173.65

ratios N/m^* are obtained. The disagreement between ε_L and ε_∞ may be due to free carriers' contribution [37]. The values of the lattice dielectric constant ε_L decrease from 4.86 to 4.09 for the annealed samples at 150˚C, 250˚C, 380˚C, 450˚C and 550˚C. The values of N/m^* also decrease from 2.34×10^{46} to 1.11×10^{46} $g^{-1}\cdot cm^{-3}$ for the annealed samples at 150˚C, 250˚C, 380˚C, 450˚C and 550˚C, respectively.

The classic dispersion theory provides the description of the variation of $n(\lambda)$ in the region of very small values of the extinction coefficient $k(\lambda)$, under negligible damping. Wemple and DiDomenico [38] [39] described the wavelength dependence of the refractive index, $n(\lambda)$, in the transparent region for various different solids by using the single-oscillator model of the form:

$$\left(n^2-1\right)=\frac{E_d E_o}{E_o^2-\left(h\nu\right)^2}, \tag{6}$$

where $h\upsilon$ represents the photon energy, E_o is the energy of the oscillator and E_d is the dispersion energy which describes the strength of the electronic transitions. The calculated values of the dispersion parameters (E_o and E_d) are obtained by plotting of $(n^2-1)^{-1}$ against $(h\nu)^2$ for the annealed Cd_2SnO_4 thin films as shown in **Figure 8**.

The calculated dispersion energies increase with increasing annealing temperature and have the values of 1.845, 1.961, 1.951, 1.848, and 2.428 eV for the annealed Cd_2SnO_4 films at 150˚C, 250˚C, 380˚C, 450˚C and 550˚C, respectively. In addition, the calculated values of the single oscillator energies are 4.973, 4.593, 4.345, 4.788, and 5.967 eV for the annealed films at 150˚C, 250˚C, 380˚C, 450˚C and 550˚C, respectively, revealing tendency of increasing with elevating the annealing temperatures. The complex dielectric constant can be given by:

$$\varepsilon^* = \varepsilon_1 - i\varepsilon_2 \quad , \tag{7}$$

where $\varepsilon_1 = n^2 - k^2$ and $\varepsilon_2 = 2nk$ are the real and imaginary parts, respectively, of the dielectric constant. The spectra of real and imaginary parts are, respectively, called dispersion and absorption curves, which are shown in **Figure 9**. It is clear that the variation of ε_1 follows the same trend as the real part of the refractive index as shown in **Figure 6**, whereas the variation of ε_2 mainly follows the behavior of k which is related to the variation of photon energy.

The real σ_1 and imaginary σ_2 parts of the optical conductivity are written as [39] [40]:

$$\sigma_1 = \omega\varepsilon_2\varepsilon_0 \quad \text{and} \quad \sigma_2 = \omega\varepsilon_1\varepsilon_0 \tag{8}$$

where ω is the angular frequency, ε_0 is the permittivity of freespace. The spectra of real and imaginary parts of the optical conductivity are shown in **Figure 10**. It can be observed that the real part of the optical conductivity

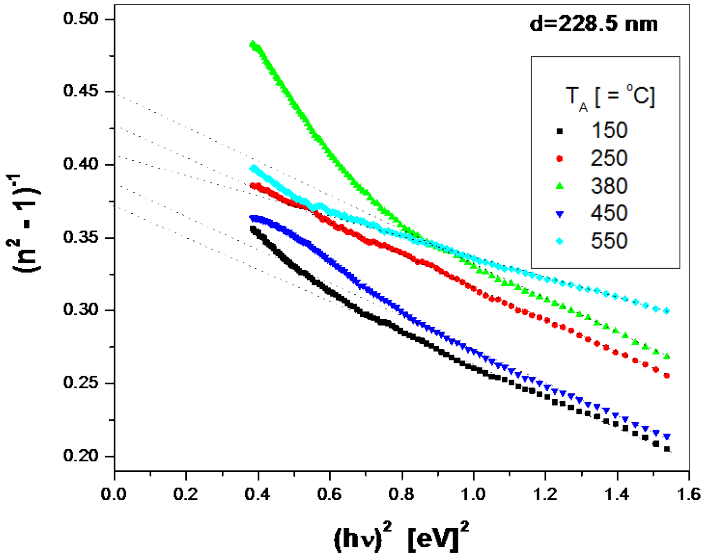

Figure 8. The relationship between $(n^2-1)^{-1}$ and $(h\upsilon)^2$ for the annealed Cd_2SnO_4 thin films.

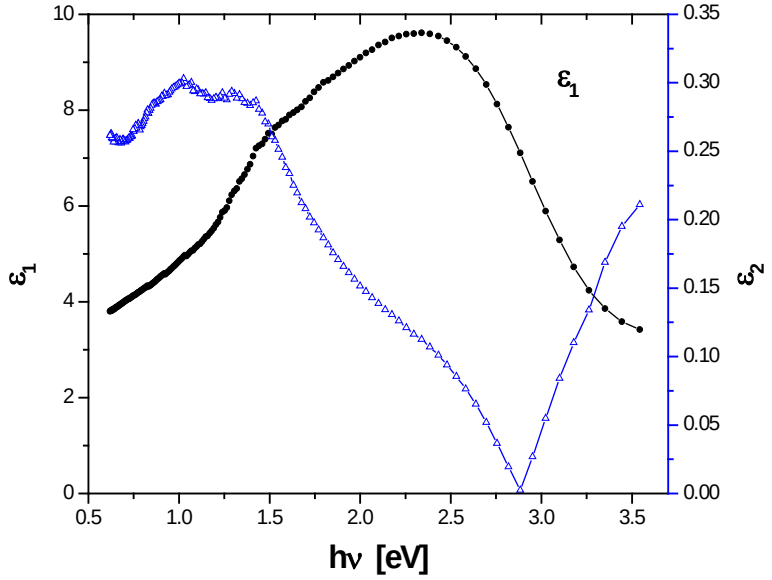

Figure 9. The spectral behaviour of the real part (ε_1) and the imaginary part (ε_2) of complex dielectric constant for the annealed Cd_2SnO_2 thin films.

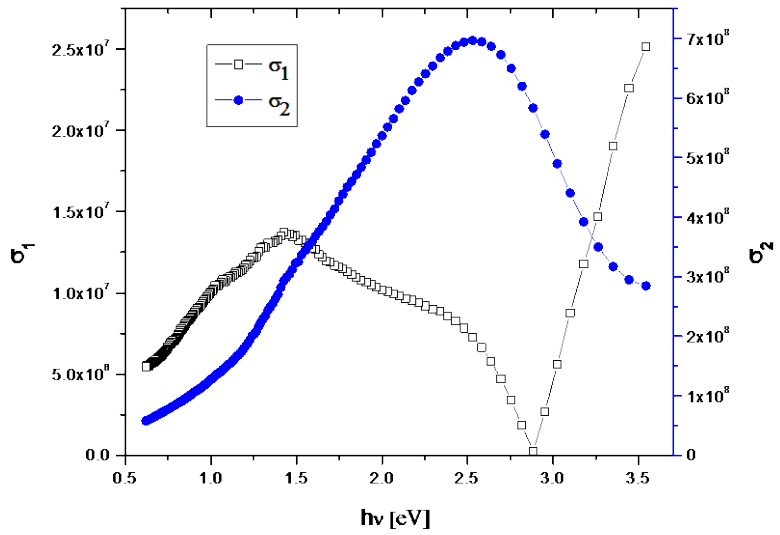

Figure 10. The spectral behaviour of the real part (σ_1) and the imaginary part (σ_2) of complex optical conductivity for the annealed Cd_2SnO_2 thin films.

σ_1 increases by increasing the energy starting from photon energy 2.9 eV. This suggests that the increase in optical conductivity is due to electrons excited by photon energy [28].

4. Conclusion

Cadmium tin oxide Cd_2SnO_4 thin films of the same thickness (228.5 nm) were prepared by RF magnetron sputtering technique on glass substrates at room temperature. AFM images revealed the change of morphology at the nanoscale with increasing annealing temperature. The optical energy gap was found to increase with increasing the annealing temperature. The width of the band tails of the localized states was found to decrease with increasing annealing temperature. The refractive index decreased with increasing the incident wavelength and with increasing annealing temperature as well. The dispersion energy was found to have the tendency of decreasing with elevating the annealing temperatures, whereas the single oscillator energy was found to increase

by increasing the annealing temperatures.

Acknowledgements

The author is thankful to Professor Mostafa M. Abdelraheem for his support throughout this work. The financial support is appreciated from the vice precedency for graduate studies and scientific research at Taif University.

References

[1] Wang, J.X., Xie, S.S., Gao, Y., Yan, X.Q., Liu, D.F., Yuan, H.J. and Wang, G. (2004) *Journal of Crystal Growth*, **267**, 177-183. http://dx.doi.org/10.1016/j.jcrysgro.2004.03.052

[2] Shannon, R.D., Gillson, J.L. and Bouchard, R.J. (1977) *Journal of Physics and Chemistry of Solids*, **38**, 877-881. http://dx.doi.org/10.1016/0022-3697(77)90126-3

[3] Omata, T., Ueda, N., Ueda, K. and Kawazoe, H. (1994) *Applied Physics Letters*, **64**, 1077-1078. http://dx.doi.org/10.1063/1.110937

[4] Wu, X., Mulligan, W.P. and Coutts, T.J. (1996) *Thin Solid Films*, **286**, 274-276. http://dx.doi.org/10.1016/S0040-6090(95)08527-0

[5] Coutts, T.J., Young, D.L., Li, X., Mulligan, W.P. and Wu, X. (2000) *Journal of Vacuum Science & Technology A*, **18**, 2646-2660. http://dx.doi.org/10.1116/1.1290371

[6] Wu, X., Dhere, R.G., Albin, D.S., Gessert, T.A., Dehart, C., Keane, J.C. and Sheldon, P. (2001) High-Efficiency CTO/ZTO/CdS/CdTe Polycrystalline Thin-Film Solar Cells. *Proceedings of NCPV Program Review Meeting*, **47**.

[7] Jayakrishnan, R. andHodes, G. (2003) *Thin Solid Films*, **440**, 19-25. http://dx.doi.org/10.1016/S0040-6090(03)00811-3

[8] Biswas, P.K., De, A., Pramanik, N.C., Chakraborty, P.K., Ortner, K., Hock, V. and Korder, S. (2003) *Materials Letters*, **57**, 2326-2332. http://dx.doi.org/10.1016/S0167-577X(02)01220-X

[9] Yamamoto, S., Yamanaka, T. and Ueda, Z. (1987) *Journal of Vacuum Science & Technology A*, **5**, 1952-1955. http://dx.doi.org/10.1116/1.574889

[10] Kobayashi, H., Mori, H., Ishida, T. and Nakato, Y. (1995) *Journal of Applied Physics*, **77**, 1301-1307. http://dx.doi.org/10.1063/1.358932

[11] Pla, J., Tamasi, M., Rizzoli, R., Losurdo, M., Centurioni, E., Summonte, C. and Rubinelli, F. (2003) *Thin Solid Films*, **425**, 185-192. http://dx.doi.org/10.1016/S0040-6090(02)01143-4

[12] Togashi, S. (1992) *Optoelectronics—Devices and Technologies*, **7**, 271.

[13] Kawachi, G., Kimura, E., Wakui, Y., Konishi, N., Yamamoto, H., Matsukawa, Y. and Sasano, A. (1994) *IEEE Transactions on Electron Devices*, **41**, 1120-1124. http://dx.doi.org/10.1109/16.293338

[14] Manifacier, J.C. (1982) *Thin Solid Films*, **90**, 297-308. http://dx.doi.org/10.1016/0040-6090(82)90381-9

[15] Southwick, R.D., Wasylyk, J.S., Smay, G.L., Kepple, J.B., Smith, E.C. and Augustsson, B.O. (1981) *Thin Solid Films*, **77**, 41-50. http://dx.doi.org/10.1016/0040-6090(81)90358-8

[16] Roos, A. (1991) *Thin Solid Films*, **203**, 41-48. http://dx.doi.org/10.1016/0040-6090(91)90514-X

[17] Sberveglieri, G., Benussi, P., Coccoli, G., Groppelli, S. and Nelli, P. (1990) *Thin Solid Films*, **186**, 349-360. http://dx.doi.org/10.1016/0040-6090(90)90150-C

[18] Matin, M.A., Jezierski, A.F., Bashar, S.A., Lacklison, D.E., Benson, T.M., Cheng, T.S. and Rezazadeh, A.A. (1994) *Electronics Letters*, **30**, 318-320. http://dx.doi.org/10.1049/el:19940243

[19] Margalith, T., Buchinsky, O., Cohen, D.A., Abare, A.C., Hansen, M., DenBaars, S.P. and Coldren, L.A. (1999) *Applied Physics Letters*, **74**, 3930-3932. http://dx.doi.org/10.1063/1.124227

[20] Chen, H.Y., Qiu, C.F., Wong, M. and Kwok, H.S. (2003) *IEEE Electron Device Letters*, **24**, 315-317. http://dx.doi.org/10.1109/LED.2003.812550

[21] Pan, S.M., Tu, R.C., Fan, Y.M., Yeh, R.C. and Hsu, J.T. (2003) *IEEE Photonics Technology Letters*, **15**, 649-651. http://dx.doi.org/10.1109/LPT.2003.809985

[22] Berger, P.R., Dutta, N.K., Zydzik, G., O'Bryan, H.M., Keller, U., Smith, P.R. and Cho, A.Y. (1992) *Applied Physics Letters*, **61**, 1673-1675. http://dx.doi.org/10.1063/1.108447

[23] Chang, S.J., Lee, M.L., Sheu, J.K., Lai, W.C., Su, Y.K., Chang, C.S. and Tsai, J.M. (2003) *IEEE Electron Device Letters*, **24**, 212-214. http://dx.doi.org/10.1109/LED.2003.812147

[24] Chopra, K.L., Major, S. and Pandya, D.K. (1983) *Thin Solid Films*, **102**, 1-46. http://dx.doi.org/10.1016/0040-6090(83)90256-0

[25] Choi, Y.S., Lee, C.G. and Cho, S.M. (1996) *Thin Solid Films*, **289**, 153-158. http://dx.doi.org/10.1016/S0040-6090(96)08923-7

[26] Stanimirova, T.J., Atanasov, P.A., Dimitrov, I.G. and Dikovska, A.O. (2005) *Journal of Optoelectronics and Advanced Materials*, **7**, 1335-1340.

[27] Al-Baradi, A.M., El-Nahass, M.M., El-Raheem, M.A., Atta, A.A. and Hassanien, A.M. (2014) *Radiation Physics and Chemistry*, **103**, 227-233. http://dx.doi.org/10.1016/j.radphyschem.2014.05.055

[28] El-Nahass, M.M., Atta, A.A., El-Raheem, M.A. and Hassanien, A.M. (2014) *Journal of Alloys and Compounds*, **585**, 1-6. http://dx.doi.org/10.1016/j.jallcom.2013.09.079

[29] Ali, H.M. (2005) *Physicastatus Solidi* (*A*), **202**, 2742-2752. http://dx.doi.org/10.1002/pssa.200521045

[30] Mamazza, R., Morel, D.L. and Ferekides, C.S. (2005) *Thin Solid Films*, **484**, 26-33. http://dx.doi.org/10.1016/j.tsf.2005.01.097

[31] Burstein, E. (1954) *Physical Review*, **93**, 632-633. http://dx.doi.org/10.1103/PhysRev.93.632

[32] Moss, T.S. (1954) *Proceedings of the Physical Society*, *Section B*, **67**, 775-782. http://dx.doi.org/10.1088/0370-1301/67/10/306

[33] Ali, H.M., El-Raheem, M.A., Megahed, N.M. and Mohamed, H.A. (2006) *Journal of Physics and Chemistry of Solids*, **67**, 1823-1829. http://dx.doi.org/10.1016/j.jpcs.2006.04.005

[34] El-Raheem, M.A., Wakkad, M.M., Megahed, N.M., Ahmed, A.M., Shokr, E.K. and Dongol, M. (1996) *Journal of Materials Science*, **31**, 5759-5764. http://dx.doi.org/10.1007/BF01160825

[35] Urbach, F. (1953) *Physical Review*, **92**, 1324. http://dx.doi.org/10.1103/PhysRev.92.1324

[36] El-Raheem, M.A. (2007) *Journal of Physics*: *Condensed Matter*, **19**, Article ID: 216209. http://dx.doi.org/10.1088/0953-8984/19/21/216209

[37] Vigil, O., Cruz, F., Morales-Acevedo, A., Contreras-Puente, G., Vaillant, L. and Santana, G. (2001) *Materials Chemistry and Physics*, **68**, 249-252. http://dx.doi.org/10.1016/S0254-0584(00)00358-8

[38] Wemple, S.H. and DiDomenico Jr., M. (1971) *Physical Review B*, **3**, 1338-1351. http://dx.doi.org/10.1103/PhysRevB.3.1338

[39] Wemple, S.H. (1973) *Physical Review B*, **7**, 3767-3777. http://dx.doi.org/10.1103/PhysRevB.7.3767

[40] Caglar, Y., Ilican, S. and Caglar, M. (2007) *The European Physical Journal B*, **58**, 251-256. http://dx.doi.org/10.1140/epjb/e2007-00227-y